Catalysis Science & Technology

Accepted Manuscript

ROYAL SOCIETY OF CHEMISTRY

www.rsc.org/catalysis

Cite this: DOI: 10.1039/c0xx00000x

www.rsc.org/xxxxxx

ARTICLE TYPE

Ozone catalytic oxidation of adsorbed benzene over AgMn/HZSM-5 catalysts at room temperature

Yang Liu[a], Xiao-Song Li[a], Chuan Shi[a], Jing-Lin Liu[a], Ai-Min Zhu[a,*], Ben W.-L. Jang[b,*]

Received (in XXX, XXX) Xth XXXXXXXXX 20XX, Accepted Xth XXXXXXXXX 20XX

DOI: 10.1039/b000000x

To provide insight into the mechanism of plasma catalytic oxidation of adsorbed benzene in a cycled storage-discharge (CSD) plasma catalytic process, ozone catalytic oxidation (OZCO) of adsorbed benzene on AgMn/HZSM-5 (AgMn/HZ) catalyst at room temperature was studied. The properties of AgMn/HZ catalyst were compared with HZ, Mn/HZ, Ag/HZ catalysts in investigations of TPD of adsorbed benzene, the product distribution and O_3 decomposition in OZCO of adsorbed benzene, and TPO and TPD of the used catalysts. For the AgMn/HZ catalyst, the adsorption capacity and the adsorption strength of benzene have been significantly improved as compared to HZ, Ag/HZ and Mn/HZ. Adsorbed benzene is oxidized completely to CO_2 by O_3 catalyzed by Ag on HZ. MnO_x, on the other hand, further speeds up the OZCO rate of benzene adsorbed on Ag/HZ.

Introduction

For removing low-concentration VOCs, the problems of high energy cost, harmful by-products (such as NO_x and CO) and poor humidity tolerance make plasma-based technique impractical.[1-4] To solve these problems, a cycled storage-discharge (CSD) plasma catalytic method was proposed by Kim et al.,[5,6] Kuroki et al.[7-9] and our group,[10-12] which operates in a cycle system composed of Storage Stage and Discharge Stage. That is, the low-concentration VOCs are first stored on catalysts at a storage stage (plasma off) and then the stored VOCs are oxidized to CO_2 by plasma at a discharge stage (plasma on).

In our previous work,[10,12] Ag supported on the high-silica HZSM-5 (HZ) catalysts exhibited not only preferential adsorption of benzene in humid air due to the hydrophobic property of the HZ support in a Storage Stage, but also almost complete oxidation of adsorbed benzene in a Discharge Stage. Moreover, ozone is a very important and long-life species in O_2 or air plasma and manganese oxide catalysts are highly active for ozone decomposition.[13-21] Therefore, to provide insight into the mechanism of plasma catalytic oxidation of adsorbed benzene, we focus on ozone catalytic oxidation (OZCO) of benzene adsorbed on AgMn/HZ catalysts in this paper.

OZCO of gaseous benzene has been reported using manganese oxides supported on SiO_2, Al_2O_3, TiO_2, ZrO_2 and Y zeolite supports[22-25] or Ag/Al_2O_3 catalyst.[26] However, to the best of our knowledge, no study has been reported to focus on OZCO of adsorbed benzene. OZCO of adsorbed benzene has two advantages over OZCO of gaseous benzene: increasing the efficiency of O_3 decomposition and reducing the second pollution caused by residual O_3 in the flue gas since O_3 decomposition would not reach 100% during OZCO of gaseous benzene at room temperature. Herein, study on OZCO of adsorbed benzene on AgMn/HZ catalyst is reported for the first time.

Experimental

Catalysts Preparation

HZ-supported catalysts were prepared via incipient wetness impregnation method using HZ (SiO_2/Al_2O_3=360) as the support. $AgNO_3$ and $Mn(CH_3COO)_2{\cdot}4H_2O$ were used as Ag and Mn precursors, respectively. The impregnated samples were stirred for 30 min, aged overnight at ambient temperature in darkness, dried at 110 ^oC for 6 h and calcined at 450 ^oC for 3 h. The obtained powders were grounded, tableted, crushed and sieved to 20-40 mesh.

ICP, BET, XPS & TPR Characterization

Inductively coupled plasma-atomic emission spectroscopy (ICP-AES, optima 2000DV, USA) was used to determine Ag and Mn loadings. The ICP-AES results are summarized in Table 1. The Ag loading of Ag/HZ catalyst was 0.7 wt% and the Mn loading of Mn/HZ catalyst was 1.8 wt%. The Ag and Mn loadings of AgMn/HZ catalyst were 0.8 wt% and 1.7 wt%, respectively.

The specific surface areas of the catalysts were measured by the N_2 adsorption BET method at 77.4 K (Autosorb-1, Quantachrome, USA). For HZ, Mn/HZ, Ag/HZ and AgMn/HZ catalysts, the BET surface areas were 341, 328, 341 and 326 m^2/g, respectively, as shown in Table 1.

The surface chemical states of the catalysts were examined by X-ray photoelectron spectroscopy (XPS, Kratos Axis Ultra DLD, UK) with a mono Al Kα X-ray source. The reference energy used

Table 1 Metal loadings, BET surface area and breakthrough capacity of the catalysts

Catalyst	Ag loading (wt%)	Mn loading (wt%)	BET surface area (m^2/g)	Breakthrough capacity[a] (μmol g-cat^{-1})
HZ	-	-	341	42.1
Mn/HZ	-	1.8	328	43.1
Ag/HZ	0.7	-	341	45.5
AgMn/HZ	0.8	1.7	326	49.1

[a] Conditions: benzene concentrations in dry simulated air were 12, 12, 11 and 10 ppm for HZ, Mn/HZ, Ag/HZ and AgMn/HZ, respectively. F=100 SCCM, GHSV= 119366 h^{-1}.

for calibration was the C 1s signal at 284.6 eV.

The redox behavior was evaluated by temperature programmed reduction (TPR) experiments on Chemisorption Analyzer (Autochem II 2920, micromeritics, USA). Firstly, 100 mg of the samples were pretreated in 50 SCCM dry air stream at 450 °C for 1 h and then cooled down to room temperature in N_2 stream. Dry simulated air was used to truly reflect the real reaction states of the silver and manganese species during benzene oxidation process, since all samples were pretreated in dry simulated air before OZCO of benzene. The TPR experiments were performed using 5% H_2 in Ar with a flow rate of 50 SCCM. The temperature was increased to 450 °C with a heating rate of 10 °C/min.

Breakthrough Capacity of Benzene, Temperature Programmed Desorption (TPD) and OZCO of Adsorbed Benzene

Fig. 1 displays the schematic diagram of the experimental setup. A quartz U-tube reactor (i.d. 4 mm) was immersed in water bath at 20 °C. Before performing the experiments, all catalysts were pretreated in a dry simulated air stream at 450 °C for 1 h and then cooled down to room temperature in N_2 stream. The breakthrough capacity (n_b, μmol/g-cat) is calculated using benzene concentration (C_{ben}, ppm), total flow rate (F, SCCM), breakthrough time (t_b, min) and mass of catalysts (m_{cat}, g):

$$n_b = \frac{C_{ben} \cdot F \cdot t_b}{22400 \cdot m_{cat}} \quad (1)$$

Benzene concentrations in dry simulated air were 12, 12, 11 and 10 ppm for HZ, Mn/HZ, Ag/HZ and AgMn/HZ, respectively. The mass of HZ, Mn/HZ, Ag/HZ and AgMn/HZ catalysts were 25.7, 26.0, 25.9 and 26.0 mg, respectively. And the total flow rate was 100 SCCM. The benzene concentration during adsorption was determined by its conversion to CO_2 using a homemade VOC-to-CO_2 converter (10%Cu/10%Mn/γ-Al_2O_3 catalysts) at 400 °C and the concentration of CO_2 was monitored online by a CO_x analyzer (S710, Sick-Maihak, Germany).[10] Breakthrough time is defined as the time when outlet concentration of benzene reached 5% of its initial concentration. The detection sensitivity of the system for benzene is 0.2 ppm.

About 53.0 mg catalyst for the TPD and OZCO of adsorbed benzene experiments was used. The dry simulated air containing about 10 ppm benzene with a total flow rate of 100 SCCM (GHSV=68209 h^{-1}) was flowed through the catalyst bed. By controlling the adsorption time, the same amount of benzene adsorbed on the four samples could be obtained and about 2.1μmol benzene was adsorbed on the catalysts. After adsorption, 200 SCCM N_2 purged for 10 min.

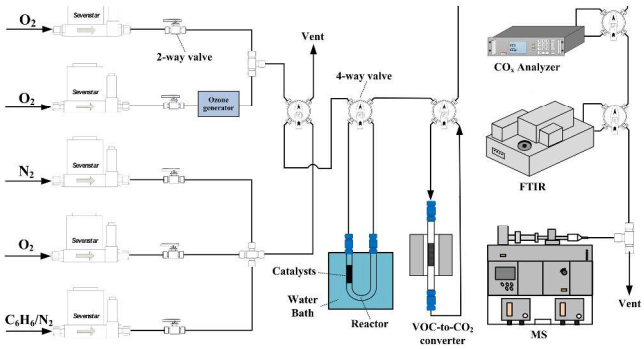

Fig.1 Schematic diagram of the experimental setup.

The TPD experiments of adsorbed benzene were heated at a ramp of 10 °C/min using N_2 as the carrier gas. The desorbed species were recorded by the online CO_x analyzer, Fourier transform-infrared (FT-IR) spectrometer (Nicolet-Antaris IGS Analyzer, Thermo, USA) and a mass spectrometer (HPR 20 QIC, HIDEN Analytical, England).

For OZCO tests, ozone was generated from O_2 by a homemade ozone generator and monitored online by FT-IR spectrometer. The flow rate of O_3/O_2 was 100 SCCM and O_3 concentration was about 211-273 ppm. In order to present how much adsorbed benzene was converted into gaseous carbon-containing species during OZCO process, carbon balance ($B^{OZCO}{}_C$) was calculated by Equation 2:

$$B_C^{OZCO} = \frac{\int_0^{t_1} F_1 C_{CO_2}^{OZCO} dt + \int_0^{t_1} F_1 C_{CO}^{OZCO} dt}{6 \times n_{ben}^{adsorbed} \times 22400} \times 100\% \quad (2)$$

where $C^{OZCO}{}_{CO2}$ and $C^{OZCO}{}_{CO}$ are CO_2 and CO concentrations (ppm) in the gas stream during OZCO process; F_1 and t_1 are the total flow rate (SCCM) and oxidation time (min) during OZCO process, respectively; $n^{adsorbed}{}_{ben}$ is the amount of benzene adsorbed on the catalysts before OZCO and equals to 2.1 μmol in this experiment.

Temperature Programmed Oxidation (TPO) and TPD of the used catalysts

TPO and TPD of the used catalysts were performed in the setup shown in Fig. 1 after purging with 90 SCCM of dry simulated air (for TPO) or N_2 (for TPD) at room temperature for over 40 min. The temperature was raised linearly at 10 °C/min. The gaseous products were analyzed by the online CO_x analyzer, FT-IR spectrometer and mass spectrometer. The total carbon balance for OZCO and TPO process ($B^{OZCO+TPO}{}_C$) is calculated to check the amount of undetected carbon-containing species during OZCO and to confirm that most of them remains on the catalyst surface:

$$B_C^{OZCO+TPO} = B_C^{OZCO} + \frac{\int_0^{t_2} F_2 C_{CO_2} dt + \int_0^{t_2} F_2 C_{CO} dt + 6\int_0^{t_2} F_2 C_{ben} dt}{6 \times n_{ben}^{adsorbed} \times 22\,400} \times 100\% \quad (3)$$

where C_{CO2}, C_{CO} and C_{ben} are CO_2 ,CO and benzene concentrations (ppm) in the gas stream during TPO process; F_2 and t_2 are the total flow rate (SCCM) and the time (min) during TPO process, respectively. Moreover, during the TPO and TPD of the used catalysts, the concentration (C_{CO2}) and MS signal (I_{44}) of CO_2 were on-line obtained simultaneously by the CO_x analyzer

and the mass spectrometer, respectively. Therefore, the concentrations of benzene (C_{ben}) and formic acid (C_{HCOOH}) in the outlet gas are calculated according to the following method.

The relationship of the mass signals at m/z = 44, 78, 46 (I_{44}, I_{78}, I_{46}) and the concentrations (C_{CO2}, C_{ben}, C_{HCOOH}) is shown by Equations (4) - (6).

$$I_{44} = \eta_{44}(\sigma_{CO_2}\beta_{44}^{CO_2}C_{CO_2} + \sigma_{HCOOH}\beta_{44}^{HCOOH}C_{HCOOH}) \quad (4)$$

$$I_{78} = \eta_{78}\sigma_{ben}\beta_{78}^{ben}C_{ben} \quad (5)$$

$$I_{46} = \eta_{46}(\sigma_{CO_2}\beta_{46}^{CO_2}C_{CO_2} + \sigma_{HCOOH}\beta_{46}^{HCOOH}C_{HCOOH}) \quad (6)$$

where η_{44}, η_{78} and η_{46} are the detection constants of the mass spectrometer at m/z = 44, 78 and 46, respectively; the total ionization cross sections for CO_2, benzene and formic acid at 70 eV (the electron beam energy used in our mass spectrometer ionizer) are σ_{CO2}=3.52×10^{-16} , σ_{ben}=1.50×10^{-15} , σ_{HCOOH}=4.83×10^{-16} cm^2;[27] according to our MS software, the ratios of the partial ionization cross section of CO_2, C_6H_6 and HCOOH generating the ion fragment with m/z = 44, 78, 46 to their total ionization cross section at 70 eV are $\beta^{CO2}{}_{44}$=0.78, $\beta^{CO2}{}_{46}$=0.0031, $\beta^{HCOOH}{}_{44}$=0.038, $\beta^{HCOOH}{}_{46}$=0.23, $\beta^{ben}{}_{78}$=0.53. Due to σ_{CO2}~σ_{HCOOH}, $\beta^{CO2}{}_{44}$ >> $\beta^{HCOOH}{}_{44}$ and C_{CO2} >> C_{HCOOH} in this experiment, Equation (4) can be simplified as,

$$I_{44} = \eta_{44}\sigma_{CO_2}\beta_{44}^{CO_2}C_{CO_2} \quad (7)$$

according to Equations (5) and (7), C_{ben} is obtained:

$$C_{ben} = \frac{\eta_{44}\sigma_{CO_2}\beta_{44}^{CO_2}}{\eta_{78}\sigma_{ben}\beta_{78}^{ben}} \cdot \frac{I_{78}}{I_{44}} \cdot C_{CO_2} = k_1 \cdot \frac{I_{78}}{I_{44}} \cdot C_{CO_2} \quad (8)$$

where k_1 was calibrated to be 2.37 in this experiment.

Formic acid concentration is calculated based on Equations (6) and (7):

$$C_{HCOOH} = \left(\frac{\eta_{44}}{\eta_{46}} \cdot \frac{\sigma_{CO_2}\beta_{44}^{CO_2}}{\sigma_{HCOOH}\beta_{46}^{HCOOH}} \cdot \frac{I_{46}}{I_{44}} - \frac{\sigma_{CO_2}\beta_{46}^{CO_2}}{\sigma_{HCOOH}\beta_{46}^{HCOOH}}\right) \cdot C_{CO_2} = \left(k_2 \cdot \frac{I_{46}}{I_{44}} - b\right) \cdot C_{CO_2} \quad (9)$$

where k_2 and b were calibrated to be 6.93 and 0.01 in this experiment, respectively.

Results and Discussion

XPS results

Ag/HZ, Mn/HZ and AgMn/HZ samples were examined via XPS to determine the oxidation states of surface species. Fig. 2 shows the XPS spectra of Ag/HZ, Mn/HZ and AgMn/HZ catalysts. The Ag $3d_{5/2}$ and Ag $3d_{3/2}$ peaks of Ag/HZ were located at 368.6 and 374.6 eV, respectively, which could be assigned to the metallic silver[28] and two manganese species could be distinguished from the Mn 2p peaks of Mn/HZ. The lower binding energies of Mn $2p_{3/2}$ and Mn $2p_{1/2}$, at 641.0 and 652.7 eV, respectively, were attributed to Mn^{3+}, and their higher binding energies, at 642.1 and 653.8 eV, respectively, were attributed to Mn^{4+}.[29] From Fig. 2c, it was found that in the case of AgMn/HZ, the binding energies of Ag 3d and Mn 2p peaks were the same as that of Ag/HZ and

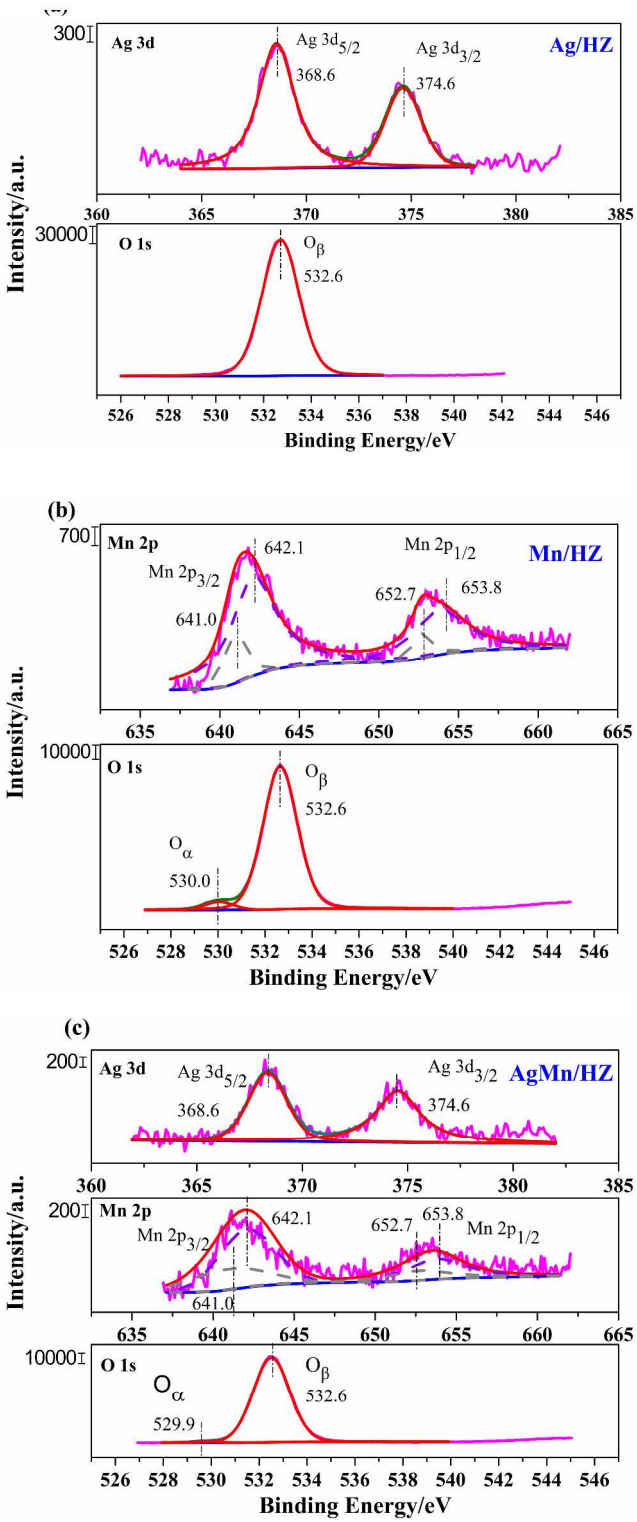

Fig. 2 XPS spectra of (a) Ag/HZ, (b) Mn/HZ and (c) AgMn/HZ catalysts.

Mn/HZ, which confirms that the silver and manganese species in AgMn/HZ were still present as metallic silver and Mn^{3+}, Mn^{4+}. Quantitative deconvolution of the Mn 2p peaks reveals that the Mn^{4+}/Mn^{3+} atomic ratios were estimated to be 5:1 and 2:1 for Mn/HZ and AgMn/HZ, respectively. This suggests that the presence of Ag favored the formation of Mn^{3+}. Two types of oxygen species were clearly distinguished on Mn/HZ and AgMn/HZ through deconvolution of the O 1s spectra (Fig. 2b and

2c). A binding energy at about 529.0-530.0 eV was ascribed to the lattice oxygen (O_α) and higher energy peak around 532.6 eV belonged to surface oxygen and OH group (O_β).[29] The area ratios of $O_\alpha/(O_\alpha+O_\beta)$ of AgMn/HZ and Mn/HZ were very low, around 0.01 and 0.04, respectively, which means that nearly all the oxygen species on Mn/HZ and AgMn/HZ presented as the form of surface oxygen and OH group. No lattice oxygen was detected on Ag/HZ, as shown in the O 1s spectra in Fig. 2a.

TPR Analysis

H_2-TPR results are shown in Fig. 3. For Mn/HZ, there was a broad peak that could be fitted into two peaks centered at 317 and 362 °C, respectively. According to the XPS data, the lower temperature peak represented the reduction of MnO_2 to Mn_2O_3. The higher temperature peak was due to the reduction of Mn_2O_3 to MnO. By curve-fitting, the area ratio between the low and high reduction peaks was about 5:6. Based on the sequential reduction steps below and the complete reduction assumption,

$$MnO_2 \xrightarrow{\frac{1}{2}H_2} \frac{1}{2}Mn_2O_3 \xrightarrow{\frac{1}{2}H_2} MnO$$

Mn^{4+}/Mn^{3+} atomic ratio of 5:1 for Mn/HZ was calculated. This result is in good agreement with the XPS data. No reduction peak was observed for Ag/HZ and this result is in good accordance with the XPS data that silver on the zeolite existed as Ag^0. Compared to the reduction behavior of Mn/HZ, for AgMn/HZ, the presence of silver led to a significant shift to lower temperature. AgMn/HZ showed two reduction peaks centered at 157 and 211 °C, which should be ascribed to the sequential reduction of MnO_2 to Mn_2O_3 and Mn_2O_3 to MnO, respectively. Because the chemical state of silver was Ag^0, Ag could not be reduced. The reduction of Mn^{4+} was enhanced by the presence of Ag, which derives from that Ag^0 might facilitate the activation (dissociation) of hydrogen and spill over of hydrogen from Ag^0 to Mn^{4+} and MnO_x dispersion in AgMn/HZ might be better than that in Mn/HZ.[30,31] The calculated Mn^{4+}/Mn^{3+} atomic ratio, using the same sequential steps as mentioned above, for AgMn/HZ based on the TPR results was 2:1, which is also consistent with the XPS results.

Breakthrough Capacity results

The breakthrough capacities of benzene on HZ, Mn/HZ, Ag/HZ and AgMn/HZ were 42.1, 43.1, 45.5 and 49.1 μmol/g-cat, respectively, as shown in Table 1. Mn/HZ possessed almost the same breakthrough capacity as HZ did which indicates that the addition of Mn species barely had an effect on the breakthrough capacity of benzene. However, the addition of Ag promoted benzene adsorption, which was due to the π-complexation adsorption of Ag with benzene.[10] AgMn/HZ possessed the highest breakthrough capacity among the four catalysts.

TPD investigation of surface adsorption site on the catalysts toward benzene

To investigate surface adsorption site on the catalysts toward benzene, TPD experiments of adsorbed benzene using N_2 as the carrier gas were conducted and the results were displayed in Fig. 4. As shown in Fig. 4a, the Mn/HZ and Ag/HZ catalysts exhibited a low-temperature benzene peak centered at about 150 °C, the same position as the desorption peak on HZ, which corresponded to desorption of benzene adsorbed on the HZ support, though the peak of Ag/HZ was much smaller than the peak of Mn/HZ which in turn was smaller than the peak of HZ. The results suggest that the addition of Mn decreased the amount of desorbed benzene on HZ slightly. On the other hand, the loading of Ag changed the adsorption of HZ significantly. The results, as shown in Fig. 4a, also suggest that there were two types of adsorption on Ag/HZ. Besides the adsorption on pure HZ support, the addition of Ag to HZ created a stronger adsorption site, likely due to π-complexation adsorption of Ag with benzene,[10] which required a much higher temperature for desorption. Whereas, for the AgMn/HZ catalyst, this low-temperature desorption peak of benzene almost disappeared, which indicates that nearly all benzene adsorbed on the Ag promoted HZ sites due to π-complexation of Ag with benzene. Instead, a high-temperature desorption peak at 420 °C occurred and was assigned to the desorption of benzene with π-complexation of Ag on HZ. Compared with the Ag/HZ catalyst, this desorption peak on AgMn/HZ shifted somewhat to higher temperature indicating an even stronger adsorption suggesting the synergetic effect of Ag with Mn in increasing the adsorption strength of benzene on HZ.

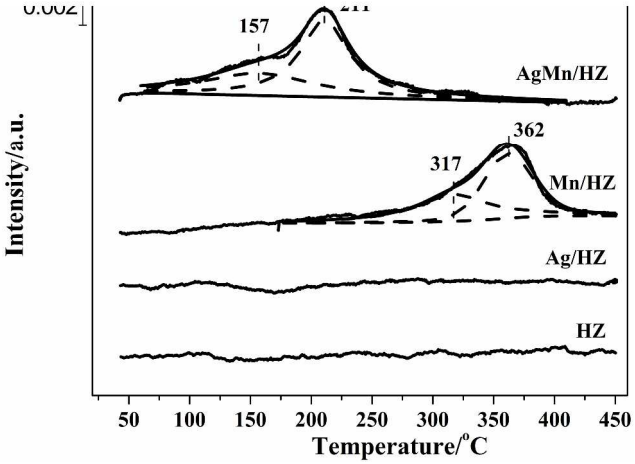

Fig. 3 H_2-TPR profiles of the catalysts. Conditions: 100 mg catalysts, 50 SCCM of 5% H_2/Ar, 10 °C/min.

Besides the desorption of benzene, on the Mn/HZ, Ag/HZ and AgMn/HZ catalysts, the adsorbed benzene was also oxidized during TPD by the surface oxygen species (adsorbed oxygen and OH group). As shown in Fig. 4b, the total amount of CO_2 evolved from Mn/HZ and Ag/HZ were 1.98 and 1.38 μmol, respectively. In addition, the peaks of CO_2 formation on the Mn/HZ and Ag/HZ catalysts occurred at 315 °C and 405 °C, respectively. This suggests that the oxidation activity of Mn/HZ was higher than Ag/HZ. On the AgMn/HZ catalyst, about 3.66 μmol CO_2 were evolved and this value is approximately equal to the sum of CO_2 evolved from Mn/HZ and Ag/HZ, which indicates that the CO_2 formation on AgMn/HZ was attributed to the oxidation of adsorbed benzene by surface oxygen species catalyzed by MnO_x and Ag. By curve-fitting the CO_2 peaks of AgMn/HZ, two peaks centered at 315 and 375 °C could be resolved (Fig. 4b inset), which were assigned to the oxidation of adsorbed benzene by surface oxygen species catalyzed by MnO_x and Ag on AgMn/HZ, respectively. Compared with Ag/HZ, the surface oxygen species

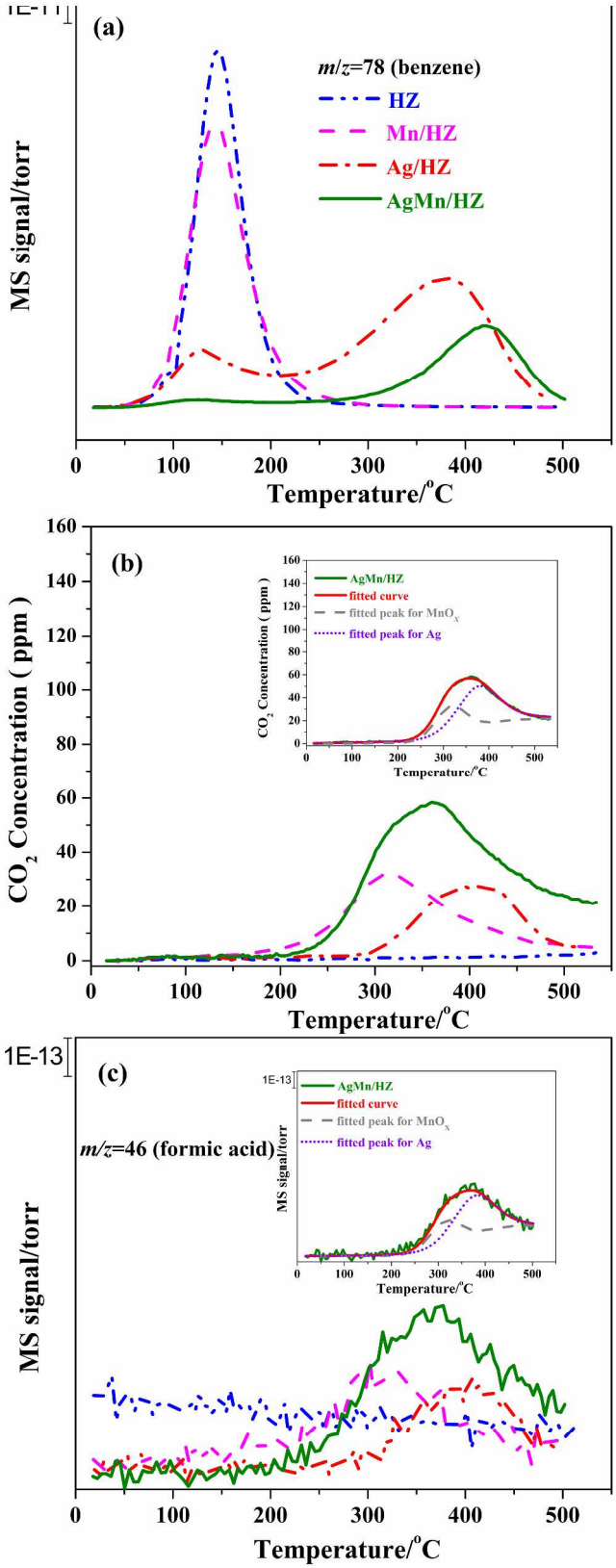

Fig. 4 TPD profiles of adsorbed benzene: (a) *m/z*=78 (benzene); (b) CO_2 concentration; (c) *m/z*=46 (formic acid). Conditions: 90 SCCM of N_2, 10 °C/min.

from Ag on AgMn/HZ were more active (because of the larger peak and the temperature shifted to a lower temperature from 405 to 375 °C). Moreover, on Mn/HZ, Ag/HZ and AgMn/HZ catalysts, small amount of formic acid evolved during the same TPD procedure (Fig. 4c). By curve-fitting the formic acid formation peaks of AgMn/HZ (Fig. 4c inset), profiles similar to those in Fig. 4b inset could be obtained. For the HZ support, no oxidation products of adsorbed benzene were detected (Fig. 4b and 4c), which indicates that Ag and Mn species are required for surface oxidation of adsorbed benzene during TPD.

OZCO of adsorbed benzene

Fig. 5a exhibits the variations of CO_2 and CO concentrations with time on stream (TOS) during OZCO of adsorbed benzene on HZ, Ag/HZ, Mn/HZ and AgMn/HZ catalysts. It should be noted that, except for CO, no other by-products were detected by the online FT-IR spectrometer for the four cases. From Fig. 5a, it could be seen that, for Ag/HZ and AgMn/HZ catalysts, no CO was produced and CO_2/CO_x reached 100% (Table 2). In contrast, for HZ and Mn/HZ catalysts, CO was detected besides CO_2 in gaseous products and CO_2/CO_x arrived at 78.4% and 87.4% at TOS = 30 min (Table 2), respectively. Thereby, it can be deduced that Ag is necessary to promote the complete oxidation of benzene to CO_2 during OZCO.

In addition, O_3 consumption, $(C^{in}_{O3}\text{-}C^{out}_{O3})/C^{in}_{O3}$ dropped quickly over HZ catalyst with or without adsorbed benzene, as shown in Fig. 5b and 5c. On HZ, O_3 consumption maintained at 100% for about 25 min, followed by a rapid decrease, as shown in Fig. 5c, which could be ascribed to the contribution of O_3 adsorption on HZ. It was reported that, ZSM-5 zeolites did not facilitate ozone decomposition but acted as ozone reservoirs on which the reaction between O_3 and the organic molecules took place[32] and possessed high capacities to adsorb O_3.[33,34] So in this paper, it is tentatively deduced that when O_3 was fed to HZ, O_3 was mainly adsorbed on HZ and then O_3 consumption began to drop rapidly after HZ was saturated. For Ag/HZ catalyst, there was some decrease in O_3 consumption after 6-min TOS in the presence of adsorbed benzene (Fig. 5b). When no benzene was adsorbed on Ag/HZ catalyst, its O_3 consumption decreased gradually after 25-min TOS (Fig. 5c). The presence of adsorbed benzene accelerated the decrease in O_3 decomposition over Ag/HZ, which was due to the adsorbed benzene decreasing the sites for O_3 adsorption. However, for Mn/HZ and AgMn/HZ catalysts, O_3 decomposition kept at 100% during the entire test with or without adsorbed benzene. This should be ascribed to very high activity of manganese oxides for O_3 decomposition.[13-21] Oyama and his co-workers[35] have reported that the decomposition of O_3 over MnO_2/Al_2O_3 catalyst without organic compounds could be described by:

$$O_3 + * \rightarrow O_2 + O^*$$
$$O^* + O_3 \rightarrow O_2 + O_2^*$$
$$O_2^* \rightarrow O_2 + *$$

where * denotes the surface site on the catalysts. O^* and O_2^* are the active species for OZCO of adsorbed benzene.[16] Moreover, it was also reported that O^* is much more stable than O_2^*.[35] Therefore, it is assumed that only one atom of O_3 was responsible for benzene oxidation and the reaction equation could be written as: $15O_3 + C_6H_6 \rightarrow 6CO_2 + 3H_2O + 15O_2$. In this paper, about 2.1μmol benzene was adsorbed on the catalysts, therefore, theoretically about 31.5 μmol O_3 is needed to oxidize all the adsorbed benzene. According to Fig. 5b, for HZ, Mn/HZ, Ag/HZ

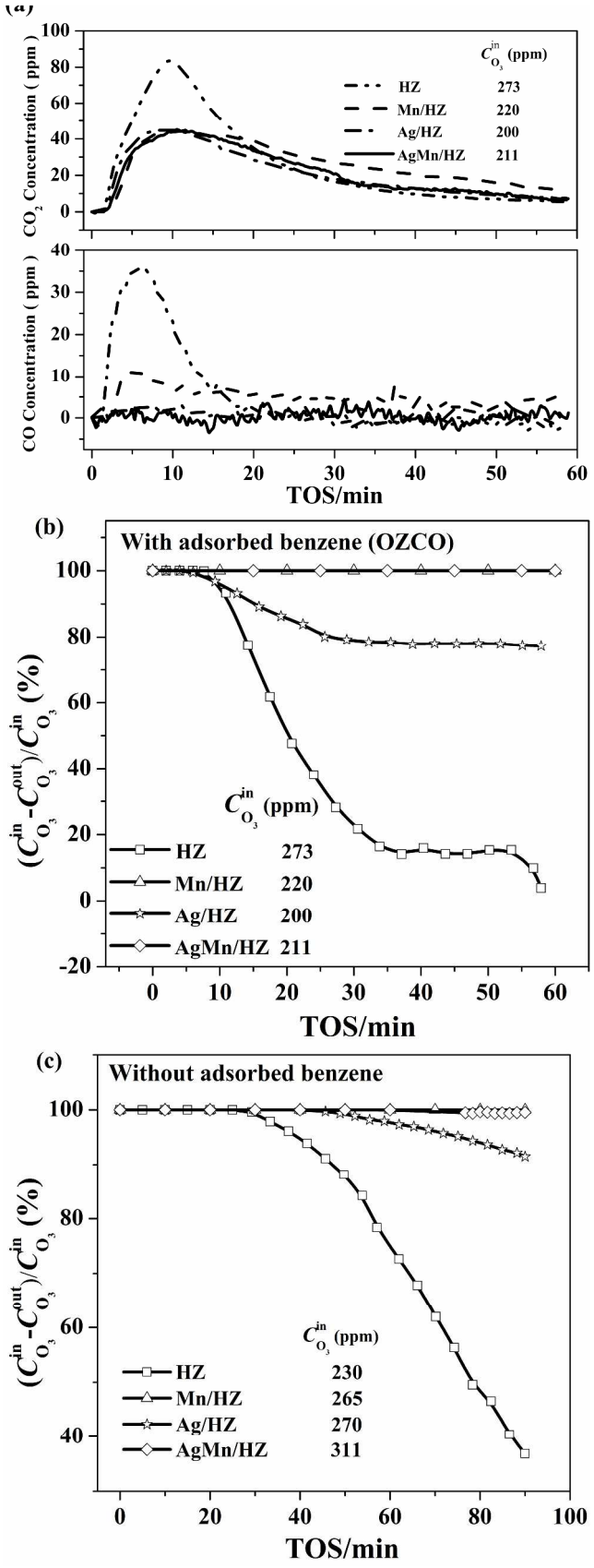

Fig. 5 (a) Time course for CO_x concentration during OZCO of adsorbed benzene; Time course for O_3 consumption (b) with and (c) without adsorbed benzene. Adsorption conditions: 2.1 μmol benzene adsorbed on the catalysts.

Table 2 Properties of the catalysts during benzene oxidation with O_3 [a]

Catalyst	CO_2/CO_x (%)	O_3 consumed (μmol)	$B^{OZCO}{}_C$ [b] (%)	$B^{OZCO+TPO}{}_C$ [b] (%)
HZ	78.4	25.6	51.6	90.3
Mn/HZ	87.4	29.5	42.1	90.0
Ag/HZ	100	23.4	31.7	89.7
AgMn/HZ	100	28.3	35.1	94.9

[a] Data in the table corresponded to 30-min TOS.

[b] The standard error was 0.3% and 0.5% for $B^{OZCO}{}_C$ and $B^{OZCO+TPO}{}_C$, respectively.

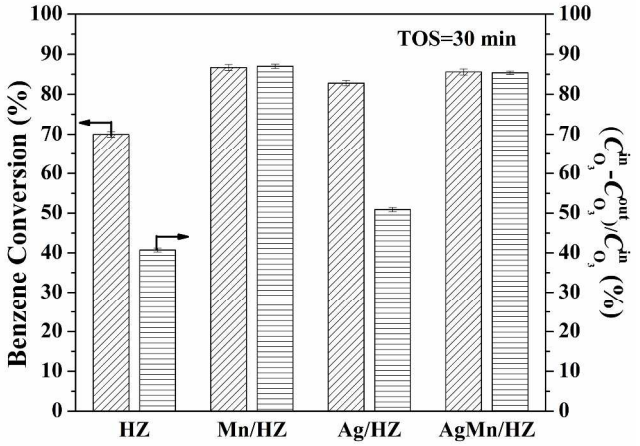

Fig. 6 Benzene conversion and O_3 consumption of HZ, Mn/HZ, Ag/HZ and AgMn/HZ during OZCO of gaseous benzene. Conditions: 53 mg catalyst, 47 ppm benzene in dry simulated air of 250 SCCM, 437-453 ppm O_3.

and AgMn/HZ, the actual amounts of O_3 consumed at TOS=30 min were 25.6, 29.5, 23.4 and 28.3 μmol, respectively. They were less than the theoretical amount of 31.5 μmol, so some amount of benzene or its derivates were still on the catalysts after 30-min OZCO. The carbon balances during OZCO, $B^{OZCO}{}_C$ at TOS=30 min were relatively low, as shown in Table 2, which were 51.6, 42.1, 31.7 and 35.1% for HZ, Mn/HZ, Ag/HZ and AgMn/HZ, respectively. However, for plasma catalytic oxidation of absorbed benzene on Ag/HZ in our previous paper,[10] carbon balance could reach about 100% within 10 min of discharge time. This confirms that, besides the contribution of ozone to benzene oxidation, there exists considerable contribution from other active species, such as electrons, UV photons, O atoms, etc.

It should be pointed out that, CO_2 concentration was higher for HZ than loaded HZ during OZCO of adsorbed benzene as shown in Fig. 5a. Similar results were also observed in our previous research. The bare HZSM-5 support produced more CO_2 during the oxidation of adsorbed benzene[10] and formaldehyde,[11] which is due to the difference in adsorption strength towards pollutants between HZ and the HZ supported catalysts. As shown in Fig. 4a, the loaded HZ catalysts possessed an even stronger adsorption of benzene. Moreover, the CO_2-TPD results by Katoh et al.[36] and Zhang et al.[37] indicated that the addition of metal into ZSM-5 caused a higher temperature CO_2 peak , which is due to the CO_2 adsorption on metal sites. Therefore, it is supported that CO_2 formed on the loaded HZ catalysts was not easy to release to gaseous phase during benzene oxidation. The lower activity of

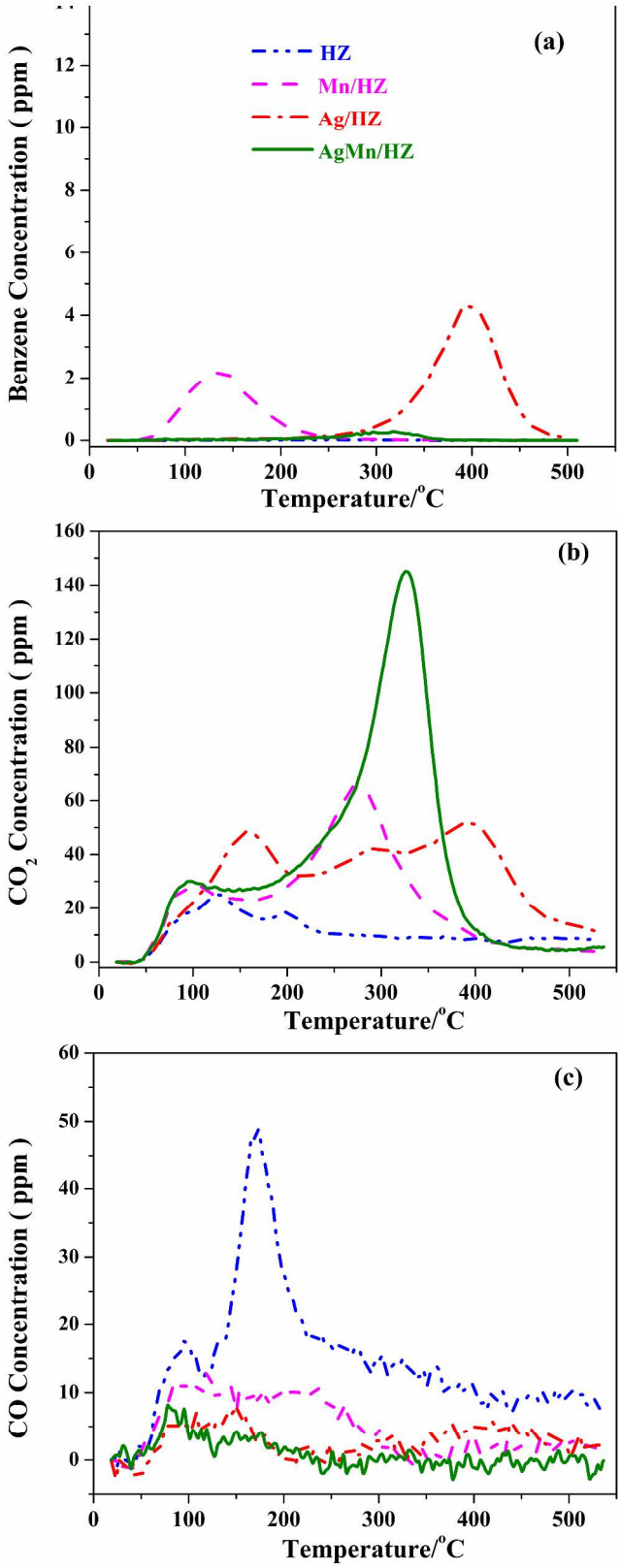

Fig. 7 TPO profiles of the used catalysts after 30-min OZCO: (a) benzene concentration; (b) CO_2 concentration; (c) CO concentration. Conditions: 90 SCCM of dry simulated air stream, 10 °C/min.

HZ and higher activity of loaded HZ during continuous OZCO of gaseous benzene are demonstrated in the additional figure (Fig. 6).

TPO and TPD investigations on surface species after OZCO of adsorbed benzene

To close the carbon balance and the surface species after OZCO as much as possible, TPO and TPD investigations were carried out on the used catalysts of OZCO of adsorbed benzene. Fig. 7 and Fig. 8 show the detailed TPO and TPD results of the used HZ, Ag/HZ, Mn/HZ and AgMn/HZ catalysts after 30-min and 60-min OZCO of adsorbed benzene, respectively. The low-temperature TPO peak of benzene on HZ and Ag/HZ catalysts disappeared completely after 30-min OZCO (Fig. 7a). But on Mn/HZ catalyst, the low-temperature peak of benzene decreased to some extent (4.8% of the adsorbed benzene was detected) (Fig. 7a) and still existed even after OZCO for 60 min (3.3% of the adsorbed benzene was detected) (Fig. 8a). It can be explained that, for O_3 decomposition, MnO_x of the Mn/HZ catalyst predominated over the HZ support. Accordingly, the probability of reaction of O_3 with benzene adsorbed on the support of the Mn/HZ catalyst decreased. For the AgMn/HZ catalyst, because there was nearly no low-temperature benzene desorption peak (Fig. 4a), therefore there was no low-temperature TPO or TPD peaks of benzene after OZCO of benzene for 30 or 60 minutes, as shown in Fig. 7a and 8a. Moreover, the high-temperature TPO peak of benzene on AgMn/HZ catalyst almost disappeared after 30-min OZCO (0.5% of the adsorbed benzene was detected), but on Ag/HZ, this TPO peak could still be observed (Fig. 7a). Even after 60-min OZCO, the high-temperature peak of benzene on Ag/HZ still existed (9.5% of the adsorbed benzene was detected) (Fig. 8a). This demonstrates that MnO_x of the AgMn/HZ catalyst causes the significant increase in oxidation rate of benzene adsorbed on Ag.

For CO_2 evolution as shown in Fig. 7b and 8b, the peaks at low temperatures (about 100 °C for Mn/HZ and AgMn/HZ and about 150 °C for Ag/HZ) corresponded to the desorption of CO_2 formed in OZCO from the HZ support; the peaks at higher temperatures (272 °C for Mn/HZ, 326 °C for AgMn/HZ and 393 °C for Ag/HZ as shown in Fig. 7b; 303 °C for Mn/HZ, 368 °C for AgMn/HZ and 397 °C for Ag/HZ as shown in Fig. 8b) were assigned to the oxidation of residual benzene and intermediate products including formates and carboxylates.[22] For the HZ support, the small peaks of CO_2 (Fig. 7b and 8b) and the large peaks of CO (Fig. 7c and 8c) located at about 180 °C derived from the decomposition of intermediate products of OZCO. Similar to Fig. 4c, in Fig. 8d, formic acid evolved with the same TPD profile as CO_2 evolution. This implies that formic acid is very likely to be an intermediate of benzene oxidation to CO_2. About 0.02, 0.08, 0.1 and 0.2 μmol formic acid were detected for HZ, Mn/HZ, Ag/HZ and AgMn/HZ, respectively. $B^{OZCO+TPO}{}_C$ for HZ, Mn/HZ, Ag/HZ and AgMn/HZ, as shown in Table 2, were increased to 90.3, 90.0, 89.7 and 94.9%, respectively. This confirms that the low $B^{OZCO}{}_C$ derived from the residual benzene or its derivates on the catalysts after OZCO of adsorbed benzene.

Conclusions

OZCO of adsorbed benzene on AgMn/HZ catalyst at room temperature was studied in comparison with that on HZ, Mn/HZ and Ag/HZ catalysts. In the gaseous products, for Ag/HZ and

AgMn/HZ catalysts, only CO_2 was detected. In contrast, for HZ and Mn/HZ catalysts, CO was formed in noticeable amount. For Ag/HZ catalyst, O_3 decomposition decreased gradually with TOS.

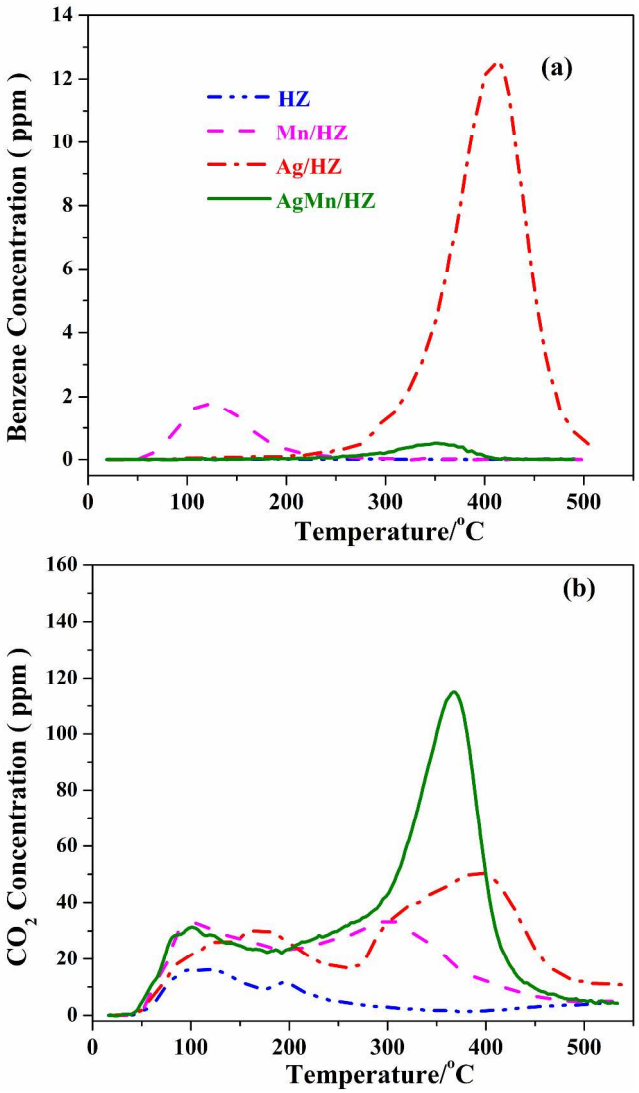

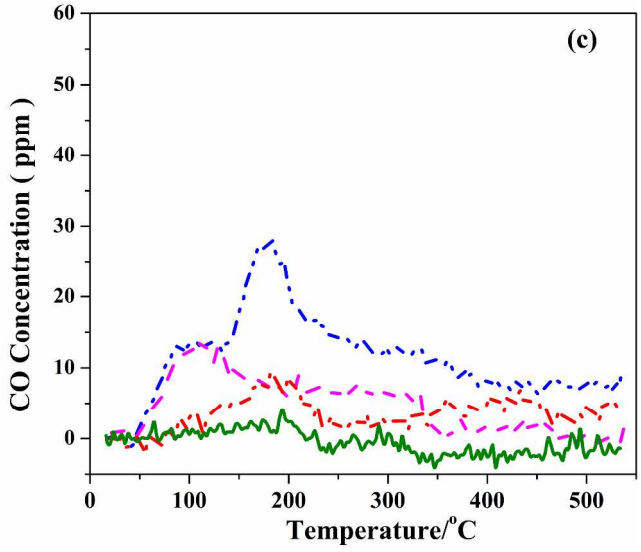

However, for Mn/HZ and AgMn/HZ catalysts, O_3 decomposition kept at 100% during the entire test with or without adsorbed benzene.

TPD investigation of adsorbed benzene demonstrated different

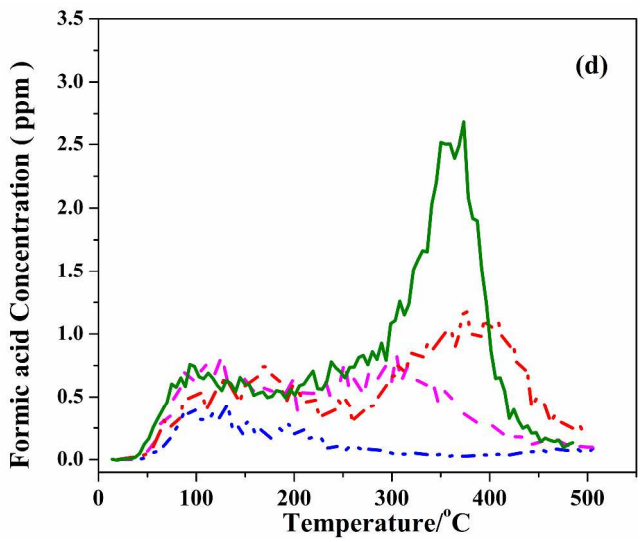

Fig. 8 TPD profiles of the used catalysts after 60-min OZCO: (a) benzene concentration; (b) CO_2 concentration; (c) CO concentration; (d) formic acid concentration. Conditions: 90 SCCM of N_2, 10 °C/min.

adsorption sites on HZ, Mn/HZ, Ag/HZ and AgMn/HZ catalysts. TPO and TPD studies of the used HZ, Ag/HZ, Mn/HZ and AgMn/HZ catalysts clarified the surface species in OZCO of adsorbed benzene. For the AgMn/HZ catalyst, the adsorption capacity and the adsorption strength of benzene have been significantly improved as compared to HZ. Adsorbed benzene is oxidized completely to CO_2 by O_3 catalyzed by Ag on HZ. MnO_x, on the other hand, further speeds up the OZCO rate of benzene adsorbed on Ag/HZ.

Acknowledgments

This work is supported by National Natural Science Foundation of China (11079013, U1201231) and Welch Foundation in US

(#T-0014).

Notes and references

[a]*Laboratory of Plasma Physical Chemistry, School of Physics and Optoelectronic Engineering & School of Chemistry, Dalian University of Technology, 116024 Dalian, China.Fax: +86-411-84706094 (A.-M. Zhu); E-mail address: amzhu@dlut.edu.cn (A.-M. Zhu).*
[b]*Department of Chemistry, Texas A&M University-Commerce, PO Box 3011, Commerce, TX 75429, United States.Fax: +1-903-468-6020 (B.W.-L. Jang);E-mail address:Ben.Jang@tamuc.edu (B.W.-L.Jang).*

1 J. Van Durme, J. Dewulf, C. Leys and H. Van Langenhove, Appl. Catal.B: Environ., 2008, **78**, 324.
2 A. Ogata, N. Shintani, K. Mizuno, S. Kushiyama and T. Yamamoto, IEEE. Trans. Ind. Appl., 1999, **35**, 753.
3 S.Ognier, S.Cavadias and J.Amouroux, Plasma Process. Polym., 2007, **4**, 528.
4 A. Ogata, K. Miyamae, K.Mizuno, S.Kushiyama and M.Tezuka, Plasma Chem. Plasma Process., 2002, **22**, 537.
5 H.H. Kim, S.M. Oh, A. Ogata and S.Futamura, J. Adv. Oxid. Technol., 2005, **8**, 226.
6 H.H. Kim, A. Ogata and S. Futamura, Appl. Catal. B: Environ., 2008, **79**, 356.
7 T. Kuroki, T. Fujioka, M. Okubo and T. Yamamoto, Thin Solid Films., 2007, **515**, 4272.
8 T. Kuroki, T. Fujioka, R. Kawabata, M. Okubo and T. Yamamoto, IEEE. Trans. Ind. Appl., 2009, **45**, 10.
9 T. Kuroki, K. Hirai, R. Kawabata, M. Okubo and T.Yamamoto, IEEE. Trans. Ind. Appl., 2010, **46**, 672.
10 H.Y. Fan, C.Shi, X.S. Li, D.Z. Zhao, Y. Xu and A.M. Zhu, J. Phys. D: Appl. Phys., 2009, **42**, 225105 (5pp).
11 D.Z. Zhao, X.S. Li, C. Shi, H.Y. Fan and A.M. Zhu, Chem. Eng. Sci.,2011, **66**, 3922.
12 H.Y. Fan, X.S. Li, C. Shi, D. Z. Zhao, J.L. Liu, Y.X. Liu and A.M. Zhu, Plasma Chem. Plasma Process., 2011, **31**, 799.
13 B. Dhandapani and S.T. Oyama, Appl. Catal.B: Environ., 1997, **11**, 129.
14 S.T. Oyama, Catal. Rev., 2000, **42**, 279.
15 D.Z. Zhao, T.Y. Ding, X.S. Li, J.L. Liu, C. Shi and A.M. Zhu, Chin. J. Catal.,2012, **33**, 396.
16 D.Z. Zhao, C. Shi, X.S. Li, A.M. Zhu and B.W.L. Jang, J. Hazard. Mater., 2012, **239-240**, 362.
17 H.C. Wang, S.H. Chang, P.C. Hung, J.F. Hwang and M.B. Chang, J. Hazard. Mater.,2009, **164**, 1452.
18 Y.F. Guo, D.Q. Ye, K.F. Chen, J.C. He and W.L. Chen, J. Mol. Catal. A: Chem.,2006, **245**, 93.
19 Y.F. Guo, D.Q. Ye, K.F. Chen and J.C. He, Catal. Today.,2007, **126**, 328.
20 E. Rezaei and J. Soltan, Chem. Eng. J.,2012, **198-199**, 482.
21 E. Rezaei, J. Soltanand N. Chen, Appl. Catal.B: Environ.,2013, **136-137**, 239.
22 H. Einaga and S. Futamura, J. Catal., 2004, **227**, 304.
23 H. Einaga and S. Futamura, Catal. Commun., 2007, **8**, 557.
24 H. Einaga and A. Ogata, J. Hazard. Mater., 2009,**164**, 1236.
25 H. Einaga, Y. Teraoka and A. Ogat, Catal. Today., 2011,**164**, 571.
26 H. Einaga and A. Ogata, Environ. Sci. Technol., 2010, **44**, 2612.
27 http://webbook.nist.gov/chemistry/form-ser.html.
28 G.I.N. Waterhouse, G.A. Bowmaker and J.B. Metson, Appl.Surf. Sci., 2001, **183**, 191.
29 C. Shi, Y. Wang, A.M. Zhu, B.B. Chen and Chaktong Au, Catal. Commun.,2012, **28**, 18.
30 S. Klacar and H. Grönbeck, Catal. Sci. Technol., 2013,**3**, 183.
31 H. Einaga, Y. Teraoka and A. Ogat, J. Catal., 2013, **305**, 227.
32 A. Ikhlaq, D.R. Brownand B. Kasprzyk-Hordern, Appl. Catal.B: Environ., 2013, **129**, 437.
33 Teresa S.C. Law, Christopher Y.H. Chao, George Y.W. Chanand Anthony K.Y. Law, Indoor Built Environ., 2004, **13**,45.
34 X. Huang, J. Yuan, J.W. Shi and W.F. Shangguan, J. Hazard. Mater.,2009,**171**, 827.
35 W. Li, G.V. Gibbs and S.T. Oyama, J. Am. Chem. Soc., 1998, **120**, 9041.
36 M. Katoh, T. Yoshikawa, T. Tomonari, K. Katayama and T. Tomida, J. Colloid Interface Sci., 2000, **226**, 145.
37 M.H. Zhang, Z.M. Liu, G.D. Lin and H.B. Zhang, Appl. Catal. A: Gen., 2013, **451**, 28.

Ozone catalytic oxidation of adsorbed benzene over AgMn/HZSM-5 catalysts at room temperature

Yang Liu[a], Xiao-Song Li[a], Chuan Shi[a], Jing-Lin Liu[a], Ai-Min Zhu[a,*], Ben W.-L. Jang[b,*]

[a]*Laboratory of Plasma Physical Chemistry, School of Physics and Optoelectronic Engineering & School of Chemistry, Dalian University of Technology, 116024 Dalian, China*

[b]*Department of Chemistry, Texas A&M University Commerce, PO Box 3011, Commerce, TX 75429, United States*

Color Graphic (8 cm × 4 cm):

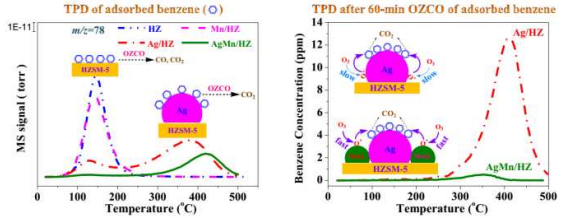

Highlight:

Investigating ozone catalytic oxidation of adsorbed benzene on AgMn/HZSM-5 to provide insight into plasma catalytic oxidation of adsorbed benzene in cycled storage-discharge process.